Adv. Polar Upper Atmos. Res., **19**, 21–41, 2005

Extreme magnetic field variations during the October 2003 superstorm

Tohru Sakurai[1*] and Yutaka Tonegawa[1]

[1] *Department of Aeronautics and Astronautics, School of Engineering, Tokai University, 1117 Kitakaname, Hiratsuka 259-1292*
[*] *Corresponding author. E-mail: sakurai@keyaki.cc.u-tokai.ac.jp*

(Received December 24, 2004; Accepted April 25, 2005)

Abstract: From October to November, 2003 the sun became very active. The plural numbers of active region appeared on the solar surface. The most prominent one was the number 486, which yielded extremely large flares X17/4B at 0951 UT on October 28, and X10/2B at 2037 UT on October 29. These big flares hurled massive coronal mass ejections (CMEs) toward the earth. In this paper the solar-terrestrial relationship during the October super magnetic storms is discussed. Two fast moving clouds of gas from the sun swept the earth and sparked extreme geomagnetic storms producing the big ground magnetic field depressions of approximately −350 nT and −400 nT of Dst.

Several interesting magnetic field variations observed in interplanetary space and their relationships to the ground magnetic field variations are discussed. Topics are as follows: 1) magnetic field polarity changes of the north-south component B_z of interplanetary magnetic field conveyed with the interplanetary coronal mass ejections (ICMEs) and their response to the magnetic field variations on the ground, 2) large amplitude tail flapping motions observed in the distant tail at about $-160\,R_e$, 3) large amplitude Pc 5 oscillations globally observed on the ground during the recovery phase of the super magnetic storm, and 4) large amplitude Pc 3 ULF waves observed in space from upstream through the magnetosheath to the dusk-side outer magnetosphere.

key words: coronal mass ejection, interplanetary magnetic field, geomagnetic storm, MHD waves

1. Introduction

Solar activity occurred on October to November 2003, that yielded violent super magnetic storms in the terrestrial magnetosphere. The magnetic activity occurred in less than a day from the beginning of the solar flares. The solar wind speed was extremely high. In order to predict the geo-effectiveness of such solar activity accurate knowledge of the solar-terrestrial relationship is desired. This storm event is a suitable example for this study. In this paper the important geomagnetic phenomena that occurred during this super magnetic storm and their relationships to solar wind features are examined in detail. In Section 2 the observed extremely high-speed solar wind and CMEs are examined. A typical relationship between ICMEs and their geo-effectiveness is discussed in Section 3. The relationships between the solar wind conditions observed by the ACE satellite in the region upstream, and tail flapping motions observed by the

WIND satellite in the distant tail downstream are examined in Section 4. Extremely large amplitude Pc 5 oscillations and their characteristics are examined in Section 5. Pc 3 pulsations (10–50 s in period) observed in interplanetary space, the magnetosheath and the dusk-side outer magnetosphere observed by the GEOTAIL satellite are examined in Section 6. Summary and discussions are described in Section 7.

2. Extremely high-speed solar wind

Large X-ray flares occurred at 0951 UT on October 28, and 2037 UT on October 29. Ejected coronal materials were hurled toward the earth, and observed in interplanetary space following shocks. The first and second shocks were observed at 0559 UT on October 29, and at 1620 UT on October 30 by ACE, at $230\,R_e$ upstream. The first shock was identified clearly accompanied with the associated shock sheath, while the second shock was not clear and did not accompany the shock sheath. During this period the WIND satellite stayed in the distant tail at $-160\,R_e$ and observed these interplanetary coronal mass ejections (ICMEs). WIND observed the first shock at 0618 UT. The second shock was not identified clearly in the magnetic field. The plasma data of both satellite, ACE and WIND were not available for this storm period. This was due to the instrument damage for these severe storms. From the observations of onsets times of flares and sscs we can estimate transit times of these shocks from the sun to the earth, which were 20.3 hrs and 20.0 hrs for the first and second shocks, respectively, which are amongst the highest speed ever observed. These observations are summarized in Table 1.

Table 1. A summary of flare onset times and shock transit times of October 2003 storm.

		1st flare	2nd flare
1	Flare onset time	0951 UT Oct 28, 2003	2037 UT Oct 29, 2003
2	Shock observed time at ACE ($230\,R_e$)	0559 UT Oct 29, 2003	1620 UT Oct 30, 2003
3	ssc onset time	0611 UT Oct 29, 2003	1637 UT Oct 30, 2003
4	Shock observed time at WIND ($-160\,R_e$)	0618 UT Oct 29, 2003	Not identified
5	Shock speed estimated from ACE and WIND arrival times	2189 km/s	Not calculated
6	Travel time from the sun to the earth	20.3 hrs	20.0 hrs
7	Shock speed estimated from travel time from the sun to the earth	2049 km/s	2193 km/s

We tried to examine a relationship between arrival times of super magnetic storms with $Dst < -200$ nT observed in this solar cycle from 1996 to 2003 and corresponding initial speeds of CMEs. The initial speeds of CMEs are employed from the LASCO CME CATALOG (http://cdaw.gsfc.nasa.gov/cme_list/). The arrival times of sscs for sampled 12 super magnetic storms and the initial speeds of the CMEs corresponding to these storms are tabulated in Table 2. The relationship is shown in Fig. 1. By taking into account of the initial speeds of the first and second CMEs of the October 2003 superstorms, the arrival times of the ssc are clearly understood to be shortest amongst the ever observed sscs. Therefore, this relationship is very useful to predict the 1 AU arrival time of ssc.

Table 2. Relationship between Halo Type CME and SSC Storm with Dst<−200 nT from 1996 to 2003.

No.	Year	SSC MM/DD/UT	Dst MM/DD	Dst (nT)	Lag time (hh:mm)	CME MM/DD	CME UT	Type	V1 (km/s)
1	1998	5/3/1743	5/4	−205	42:03	5/1	2340:09	Halo	585
2	2000	4/6/1640	4/7	−288	48:08	4/4	1632:37	Halo	1188
3	2000	7/15/1439	7/16	−301	27:45	7/14	1054:07	Halo	1674
4	2000	8/11/1846	8/12	−235	50:16	8/9	1630:05	Halo	702
5	2000	9/17/1316	9/17	−201	31:58	9/16	0518:04	Halo	1215
6	2001	3/31/0052	3/31	−387	38:26	3/29	1026:05	Halo	942
7	2001	4/11/1345	4/11	−271	32:15	4/10	0530:00	Halo	2411
8	2001	11/6/0152	11/6	−288	32:17	11/4	1635:05	Halo	1810
9	2001	11/24/0555	11/24	−221	33:25	11/22	2030:05	Halo	1437
10	2003	10/29/0611	10/30	−363	18:41	10/28	1130:05	Halo	2459
11	2003	10/30/1637	10/30	−401	19:43	10/29	2054:05	Halo	2029
12	2003	11/20/0804	11/20	−472	47:14	11/18	0850:05	Halo	1660

Lag time (hh:mm)＝SSC Onset Time−Observed Time of V1.
V1 (km/s): Initial speed of Halo Type CME.

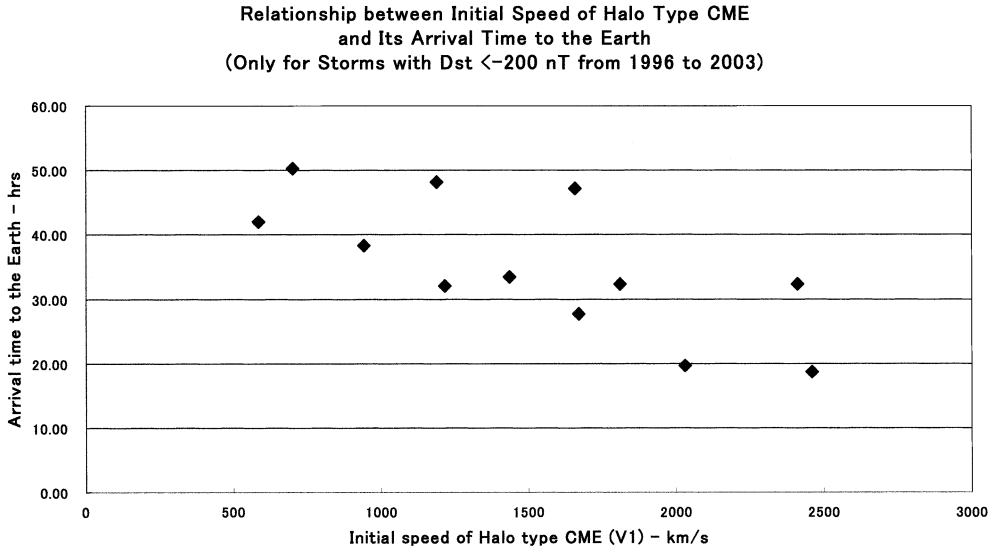

Fig. 1. The relationship between the arrival times of superstorms (Dst<−200 nT) and the initial speeds of the corresponding Halo type CMEs.

3. Field rotations of ICMEs and corresponding geomagnetic disturbances

Figure 2 shows the ICMEs successively observed by ACE on October 29–30, which is a typical example of ICME observed in interplanetary space. Clear field rotations of IMF can be seen. The first shock was observed at 0558 UT on October 29, accompanied with a sharp increase of the magnetic field intensity, and also followed by the shock sheath, in which the magnetic field varied violently, and thereafter the ICME

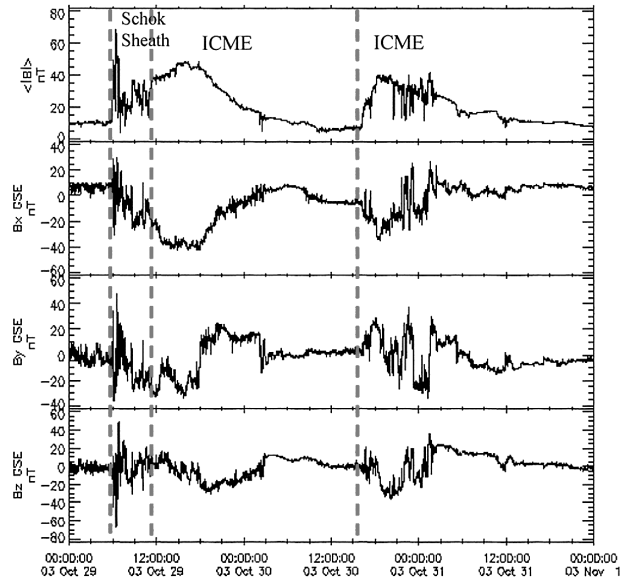

Fig. 2. The ICMEs observed by ACE at 230 R_e upstream in the super magnetic storm period from October 29 to 31, 2003. From the top to bottom panels are the magnetic field intensity, and three components of the magnetic field in the GSE coordinates. The field rotations are clearly identified in all of the components.

exhibited again clear field rotations. In particular, the north-south component of the magnetic field, B_z showed a clear field rotation from northward to southward. The other two field components, B_x and B_y also showed clear field rotations, *i.e.*, from earthward to sunward for the B_x component, and from westward to eastward for the B_y component, respectively. These field rotations continued until 03 UT on October 30 while the first ICME passed the earth. The second shock arrived at 1618 UT on October 30. Its shock sheath was not clearly identified. The body of the second ICME arrived immediately after the second shock. The magnetic field also clearly rotated from southward to northward for the B_z component, earthward to sunward for B_x and westward to eastward for B_y, respectively.

These successive ICMEs produced big geomagnetic disturbances in the terrestrial magnetosphere. This is shown in Fig. 3, which shows the geomagnetic disturbances observed at the IMAGE chain magnetometer stations (http://www.ava.fmi.fi/image/index.html). The storm sudden commencement (ssc) was observed at 0611 UT at all of the stations, indicating the shock arrival at the ground. After the first ssc the geomagnetic field showed disturbances, in particular, from 0800–1000 UT on October 29, 2003. There were some negative bay signatures at high latitude stations. This might be caused by fluctuation of IMF B_z around 0 nT. Then the activity remained quiet for a while. This is due to the geo-effectiveness for the north–south component of the IMF B_z, almost zero. That continued for about 9 hrs until 15 UT on October 29. Around 15 UT the IMF B_z turned negative and geomagnetic activity became active, *i.e.*, substorm activity began to develop and continued for about 12 hrs. Around 03 UT on

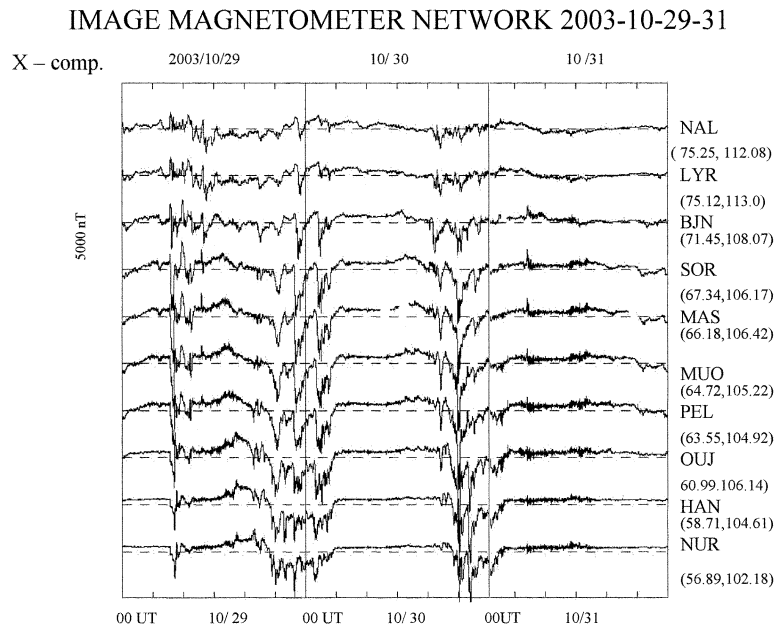

Fig. 3. The magnetic field variations observed at IMAGE chain stations during the October 2003 super storm.

October 30 the IMF B_z turned positive, and then, geomagnetic activity subsided and remained quiet until 15 UT. At that moment the second ICME passed past the earth. The large negative IMF B_z followed. The geomagnetic field then became active again, while enhanced substorm activity that continued for about 8 hrs. Around 00 UT on October 31 the IMF B_z turned positive. Geomagnetic activity suddenly subsided again. However, thereafter the activity of ULF pulsations enhanced. Large amplitude Pc 5 waves were observed during this period.

Therefore, a clear relationship between the field rotation of the IMF B_z component and geomagnetic activity existed throughout this storm. It is evident that the behavior of the IMF B_z primarily controls geomagnetic field activities although specific features in the magnetosphere are controlled by the other solar wind parameters examined in the following sections.

4. Tail flapping oscillations

During the super magnetic storm of October 29–31 WIND stayed in the nightside distant tail at about $X = -160 R_e$, where WIND measured large amplitude tail flapping oscillations as shown in Fig. 4. The oscillations were exhibited only in the X component of the magnetic field as indicated with solid circles. The lack of oscillations in the B_y and B_z components suggests that the oscillation was confined to the magnetic field, oriented parallel to the sun-earth line in a X–Z plane. The period of the oscillations was 10–30 min. The peak-to-peak amplitude was about 30–40 nT, and the oscillations were

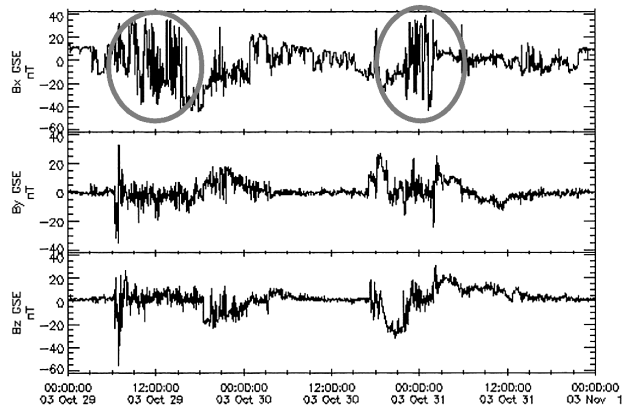

Fig. 4. The WIND observation of the magnetic field variations during the storm period. From the top to bottom panels are B_x, B_y and B_z components of magnetic field in the GSE coordinates. Large amplitude tail flapping oscillations are exhibited only in the B_x component indicated with two circles.

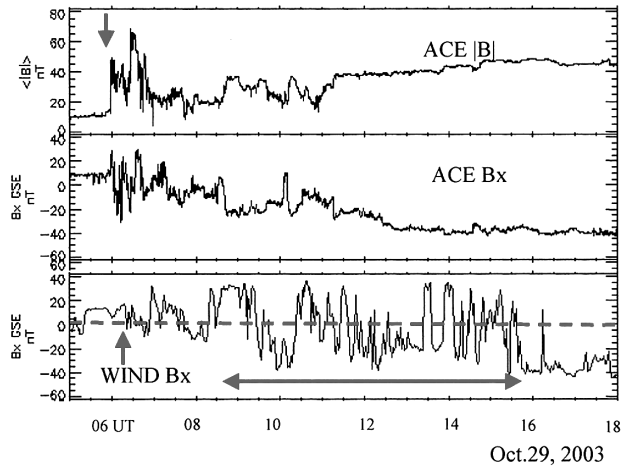

Fig. 5. The tail flapping oscillations observed by WIND at $-167\,R_e$ immediately after passing of the first ICME. No oscillations observed by ACE upstream at $230\,R_e$.

quite symmetric about $B_x=0$, which means the boundary displacements associated with this oscillation were in equal magnitude and direction. Therefore, the oscillation mode corresponds to the anti-symmetric mode by Siscoe (1969). He pointed out that this oscillation mode is similar to a rigid oscillation of the outer boundary about a central line.

In order to clarify their characteristics in detail, the oscillations exhibited in the WIND magnetogram are compared with the magnetic field variations measured by the ACE satellite located at about $230\,R_e$ upstream of the bow shock. Figure 5 shows that there are no periodic oscillations in the magnetic field intensity, $|B|$, and the X

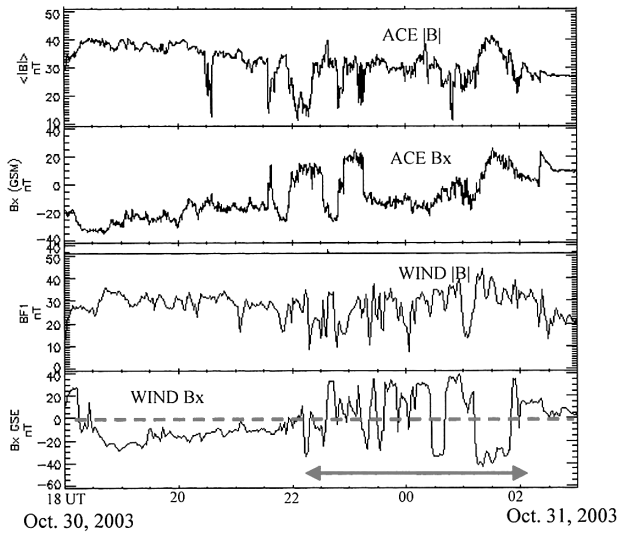

Fig. 6. The tail flapping oscillations observed by WIND immediately after passing of the second ICME. The upper and lower two panels indicate the magnetic field variations of the intensity and the B_x component in the GSE coordinates observed by ACE and WIND, respectively.

component of the magnetic field, B_x, of the ACE magnetograms, as shown in the upper panel of the figure. The bottom panel shows the oscillations, which are identified only in the B_x component of the magnetogram observed by WIND with the period of about 10–30 m. The oscillations continued from 08 UT to 16 UT on October 29 as indicated with a horizontal arrow. This oscillation occurred immediately after the passing of the first shock by WIND.

Another example of such oscillations was observed immediately after the second shock as shown in Fig. 6, in which the magnetic fields observed by ACE and WIND are given in the upper and the lower panels, respectively. In the upper panel there are no clear oscillations of the magnetic field intensity and X component at ACE. In the lower panel the oscillations are clearly identified in the X component from 22 UT on October 30 to 02 UT on October 31 as indicated with a horizontal arrow. The magnetic field of the X component varied with a period of about 10–30 m and amplitude of $\pm$30–40 nT. Moreover, the oscillation was symmetric about $B_x = 0$, suggesting that the oscillation is anti-symmetric about the central line.

5. Large amplitude Pc 5 oscillation

During the recovery phase of the super magnetic storm, IMF B_z continued northward with the amplitude of about 20 nT. In this period ULF wave activity became active. In particular, two intervals of large amplitude Pc 5 oscillations were observed from 0537 to 0740 UT, and from 11 to 14 UT. Figure 7 shows a typical example of such large amplitude Pc 5 oscillations observed at a high latitude station,

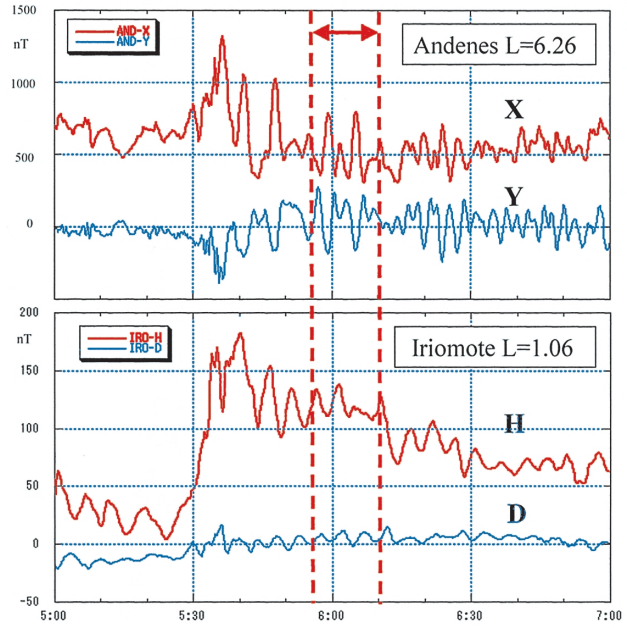

Fig. 7. Comparison of Pc 5 magnetic field oscillations, X and Y components (upper panel) at a high latitude station, Andenes (L=6.26) and H and D components (lower panel) at a low latitude station, Iriomote (L=1.06). Pc 5 oscillations were observed similarly between them. The interval of vertical dotted lines is used for a calculation of power spectrum shown in Fig. 8.

Andenes (geomag. latitude=66.5°N, geomag. long.=100.4°E), as a representative station of the Image chain stations in the auroral zone, and a low latitude station, Iriomote (geomag. lat.=13.6°N, geomag. long.=193.6°E). The Pc 5 oscillations were observed simultaneously at both stations, suggesting that this Pc 5 oscillation might be excited over a large scale in latitude and longitude from high to low latitude and from early morning to evening. Iriomote was located in the evening side at this local time. Power spectra are shown in Fig. 8 for an interval of 15 m from 0555 UT to 0610 UT as indicated with the vertical lines in Fig. 7. The Pc 5 spectral peak occurs at about 4 mHz at both stations.

From these observations we can summarize that large amplitude Pc 5 oscillations can be simultaneously observed over a large range of latitude and longitude with a similar spectral frequency of about 4 mHz. The important characteristics for this Pc 5 event are the large amplitude and the long period oscillations. The reason why this Pc 5 occurred with such a large amplitude and with such a long period is a question. We surveyed the solar wind parameters at this moment. Figure 9 shows the solar wind parameters observed by ACE during this interval, in which the solar wind proton density, solar wind bulk speed and B_z component of the magnetic field are given in the upper, middle and lower panels, respectively. Two successive solar wind density enhancements were observed during the northward IMF B_z approximately at 0500 UT and 1020 UT. The density jumps were from 1 #/cc to 4 #/cc, and from 1 #/cc to 10

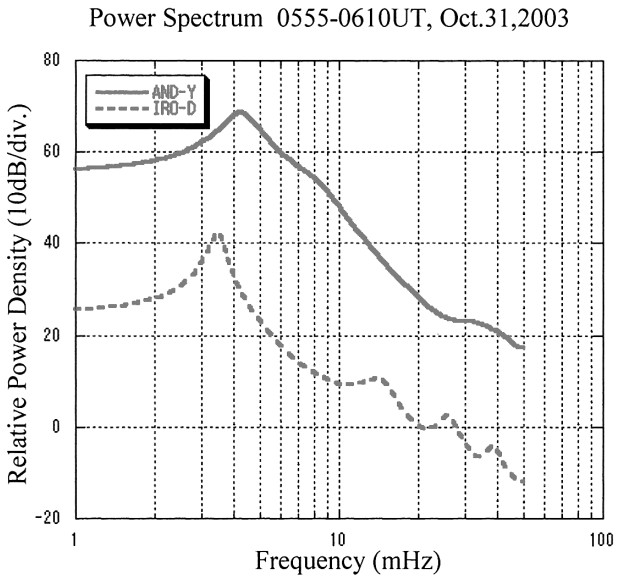

Fig. 8. Comparison of power spectra of the Y and D component magnetic field Pc 5 oscillations during the interval of 15 min from 0555 UT to 0610 UT indicated with the dotted vertical lines in the previous figure, observed at Andenes (solid curve) and Iriomote (dotted curve). Spectral peaks stand at about 4 mHz. However, the power is larger with approximately 20 dB at Andenes compared with that at Iriomote.

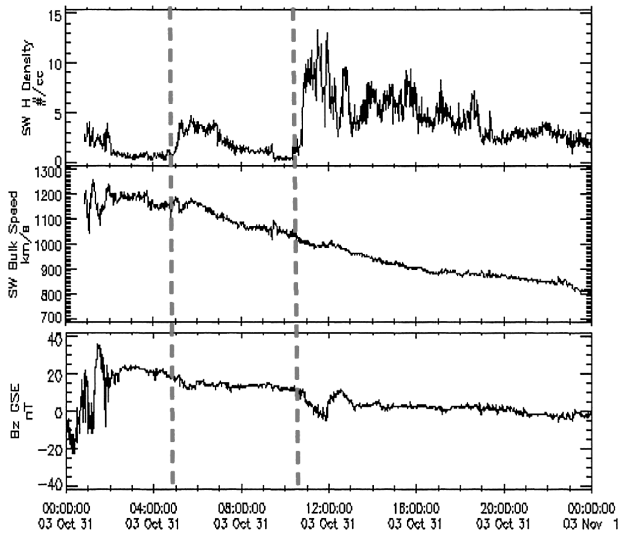

Fig. 9. Solar wind density enhancements (top panel) observed by the ACE satellite, indicated with the dashed lines at the times, 0500 UT and 1030 UT during the northward IMF, B_z (lower panel). The variation of the solar wind bulk speed is shown in the middle panel.

#/cc for the first and second case. The second density enhancement was severer and continued for a longer period.

Therefore, we can suppose that these Pc 5′s might be triggered by sudden compressions of the magnetosphere due to the sudden enhancements of solar wind density. Moreover, these Pc 5 events occurred during the recovery phase of the storm in the prevailed intense northward IMF B_z. From the turning of IMF B_z to northward at 00 UT on October 31 ULF wave activity became enhanced. Furthermore, the Dst index attained −350 nT and −400 nT for the first and second storms, respectively, suggesting that the ring current developed during these storms. Therefore, heavy ions might be expected to be injected into the inner magnetosphere during the main phase. These solar wind and magnetospheric conditions seem to be essential for triggering these large amplitude and long period Pc 5 in the magnetosphere. Therefore, we can conclude that these Pc 5′s happened to occur when these conditions are matched in between the solar wind and the magnetosphere by chance.

6. Pc 3 ULF waves observed in the foreshock, magnetosheath and outer magnetosphere

Another topic related to this storm is an intense Pc 3 ULF wave activity observed by GEOTAIL in space. During later phase of the first ICME, when the IMF was strongly northward, the GEOTAIL satellite traversed from the upstream region of the quasi-perpendicular shock, through the dusk-side magnetosheath and to the outer magnetosphere. Large amplitude Pc 3 waves were observed throughout the trajectory

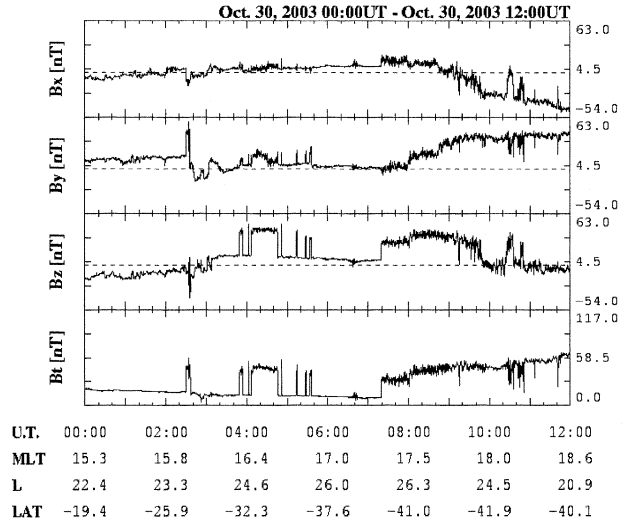

Fig. 10. An overview of the magnetic field variations observed in the upstream region to the dusk-side outer magnetosphere along the GEOTAIL satellite trajectory during the interval of 12 hrs from 0000 UT to 1200 UT on October 30. From top to bottom the panels are three components of the magnetic fields, B_x, B_y, and B_z in GSM coordinates, and the magnetic field intensity, respectively.

of GEOTAIL. The peak-to-peak amplitude was approximately 3 nT in the upstream region, and 6–7 nT in the magnetosheath and in the outer magnetosphere. The observed characteristics of the Pc 3 waves are summarized as follows: (i) The dominant frequency was observed at 20–30 mHz. (ii) The spectral peak power was approximately $5\times10\,nT^2/Hz$ in the upstream region, $8\times10\,nT^2/Hz$ in the magnetosheath and $1.5\times10^2\,nT^2/Hz$ in the outer magnetosphere. (iii) The dominant oscillation was different in each region; transverse in the upstream and the magnetosheath region near the bow shock, and compressional in the magnetosheath near the magnetopause and in the outer magnetosphere. (iv) Wave energy propagated earthward and duskward, perpendicular to the magnetic field-line with the Poynting flux of approximately $3–4\times10^{-6}\,W/m^2$ on average.

Figure 10 shows the observed magnetic field variations from 00 h to 12 h UT on October 30, when the satellite traversed upstream of the quasi-perpendicular shock to the dusk-side outer magnetosphere. Three components of magnetic field, B_x, B_y and B_z in the GSM coordinates, the magnetic field intensity, B_t, are presented from the top to the bottom panels, respectively. Multiple crossings of the bow shock are observed from 02 UT to 06 UT, which are characterized by impulsive or rectangular sudden changes in the magnetic field variations. Pc 3 ULF waves are recognized throughout the interval.

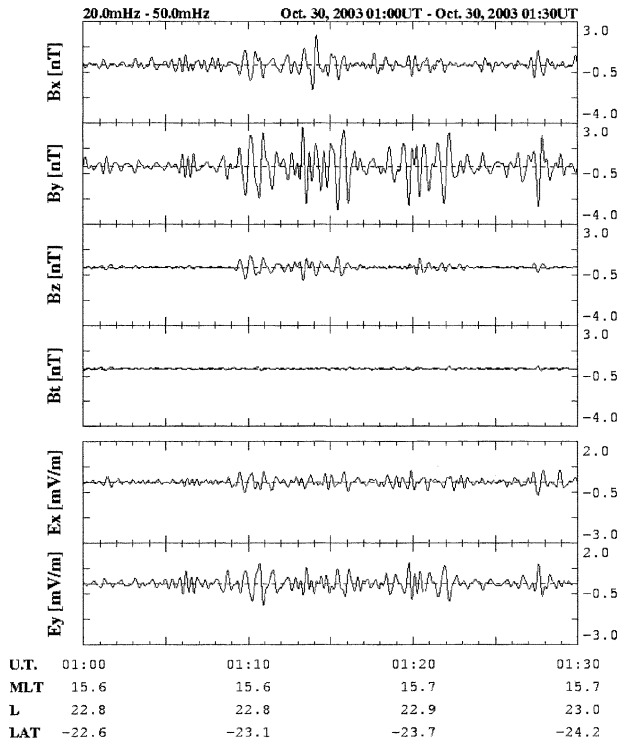

Fig. 11. A typical example of Pc 3 oscillations observed in the upstream region. The transverse oscillation is clearly identified with the largest oscillations in the B_y component of the magnetic field in the MFA coordinates.

They appear as being crowded with high-frequency variations. In particular, the large amplitude oscillations are clearly recognized in the later phase from 07 UT, when the satellite passed through the dusk-side magnetosheath and the outer magnetosphere. The observed characteristics of Pc 3 waves in each region are presented in order as follows.

An example of Pc 3 waves seen upstream of quasi-perpendicular shock is shown in Fig. 11 with representing traces of filtered Pc 3, band-pass filtered from 20 mHz to 50 mHz, from 0100 UT (1536 MLT) to 0130 UT (1542 MLT). From the top to bottom panels are three components of the magnetic field and two components of the electric field. The traces are presented with the field-aligned coordinates (MFA), in which the Z axis is parallel to the local mean-magnetic field, which is calculated every 10 min. The Y axis is taken in a plane perpendicular to the plane containing the satellite and the center of the earth. The X axis is set to the direction of a vector product between Y and Z axes. The horizontal axis of the figure indicates universal time (UT), magnetic local time (MLT), L-values and magnetic latitude (LAT). Tick marks are given each minute with a large mark at every 10 min. The Pc 3 oscillations seem to be coherent in

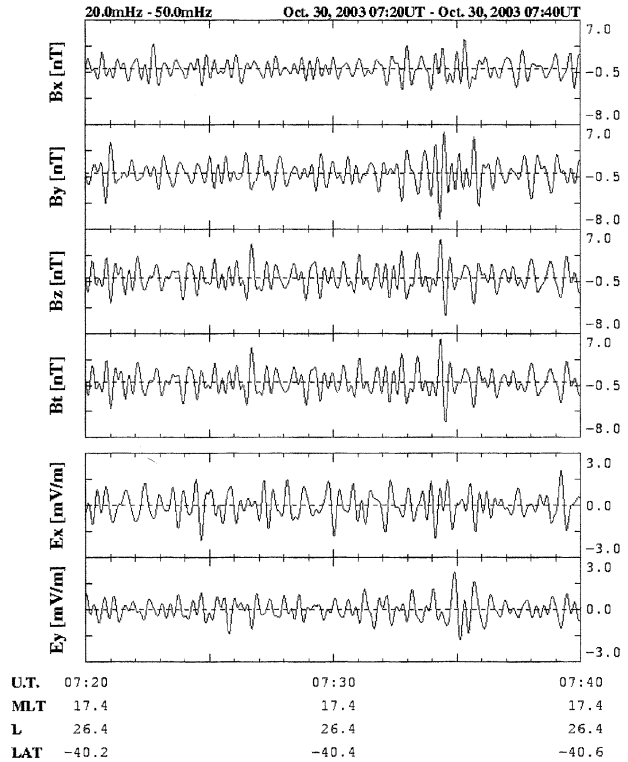

Fig. 12. A typical example of Pc 3 oscillations observed in the magnetosheath immediately after the bow shock crossing during the interval of 20 min from 0720 UT to 0740 UT. The large amplitude oscillations (6–8 nT in peak-peak) are clearly observed in all components of the magnetic field, and in the magnetic field intensity.

both fields. The largest amplitude oscillations are seen in the B_x and B_y components of the magnetic field, attaining 6–7 nT peak to peak in the B_y component. For the electric field the peak to peak amplitude is 2 mV/m in the E_y component. Therefore, the oscillations are known as transverse oscillations.

Figure 12 shows traces of the magnetic and electric field variations during the period of 20 min from 0720 UT to 0740 UT (1724 MLT) when the satellite traversed through the dusk-side magnetosheath immediately after crossing the bow shock. The peak-to-peak amplitude of the oscillation is 6–7 nT, almost the same for the three components of magnetic field. Therefore, the magnetic field oscillation exhibits both transverse and compressional modes. The electric field oscillates coherently to the magnetic field oscillation with amplitude of 2–3 mV/m. The power spectra of the magnetic field are shown in Fig. 13. From the figure two dominant spectral peaks can be recognized at 30 mHz and 60 mHz. These spectral peak powers are approximately same in both oscillation components, B_y and B_z, with the power of $7 \times 10\,\mathrm{nT}^2/\mathrm{Hz}$.

Another interval is examined for 15 min from 0740 UT to 0755 UT when the satellite stayed in the magnetosheath closely to the magnetopause. The filtered traces of three components of the magnetic field and two components of the electric field are shown in Fig. 14. Inspecting the figure the oscillation amplitude is largest in the B_z component. The peak-to-peak amplitude is about 7–8 nT. While, for the transverse components the amplitude is 3–5 nT on average. Therefore, the dominant oscillation changed to the oscillation parallel to the magnetic field-line, which means the compressional mode.

The Poynting flux is given in Fig. 15. The Poynting flux reaches approximately to

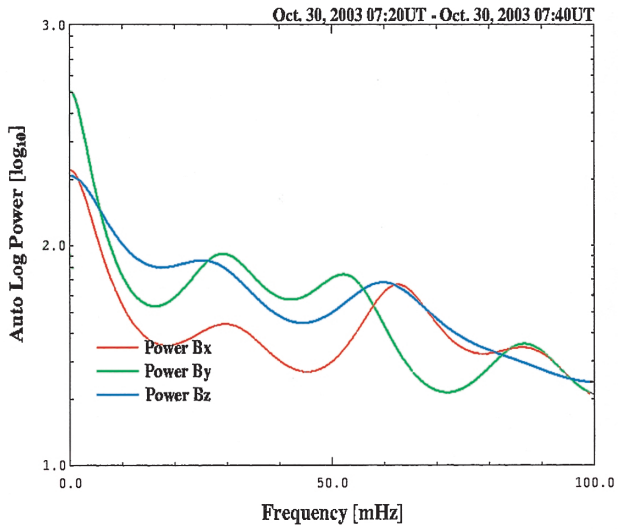

Fig. 13. Power spectra of Pc 3 for the interval of 20 m from 0720 to 0740 UT. Two spectral peaks can be identified in each field component at the frequency of 30 mHz and 60 mHz, respectively. The spectral powers of the transverse (B_y) and compressional (B_z) components are almost same.

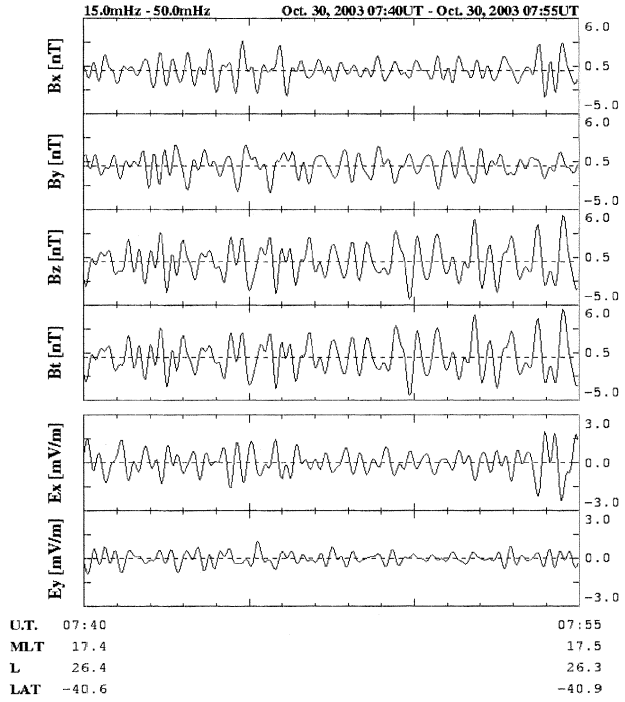

Fig. 14. A typical example of Pc 3 oscillations observed in the magnetosheath close to the magnetopause. The compressional component of the magnetic field, B_z is superior to the other two transverse components, B_x, and B_y, and extends to approximately 6–7 nT on average.

$1–2\times10^{-6}$ W/m^2. Comparing the perpendicular (S_{perp}) and parallel (S_z) components with respect to the mean magnetic field, the perpendicular component was superior to the parallel one, suggesting that the wave energy propagates dominantly perpendicular to the magnetic field-line. The direction was duskward.

Then, the satellite crossed the magnetopause at approximately 0800 UT (1730 MLT). In this case the magnetopause crossing was not clearly identified. This might be masked by the prevailing northward orientation of the IMF, B_z. The Pc 3 oscillations were, however, clearly identified in this region as shown in Fig. 10. The wave trace given in Fig. 16 was for a 30 min interval from 0810 UT to 0840 UT when the satellite stayed in the duskside outer magnetosphere immediately after crossing the magnetopause. The peak to peak amplitude of the Pc 3 was approximately 6–7 nT in the field-aligned component of the magnetic field, B_z, and 5–6 nT in the transverse components, B_x and B_y. The oscillation was characterized by the compressional mode, almost the same seen in the magnetosheath near the outside of the magnetopause. The dominant power was 1×10^2 nT^2/Hz at the frequency of 30 mHz in the compressional component, B_z. The Poynting flux was approximately $2–3\times10^{-6}$ W/m^2 and dominant in the perpendicular component, whose propagation was tailward.

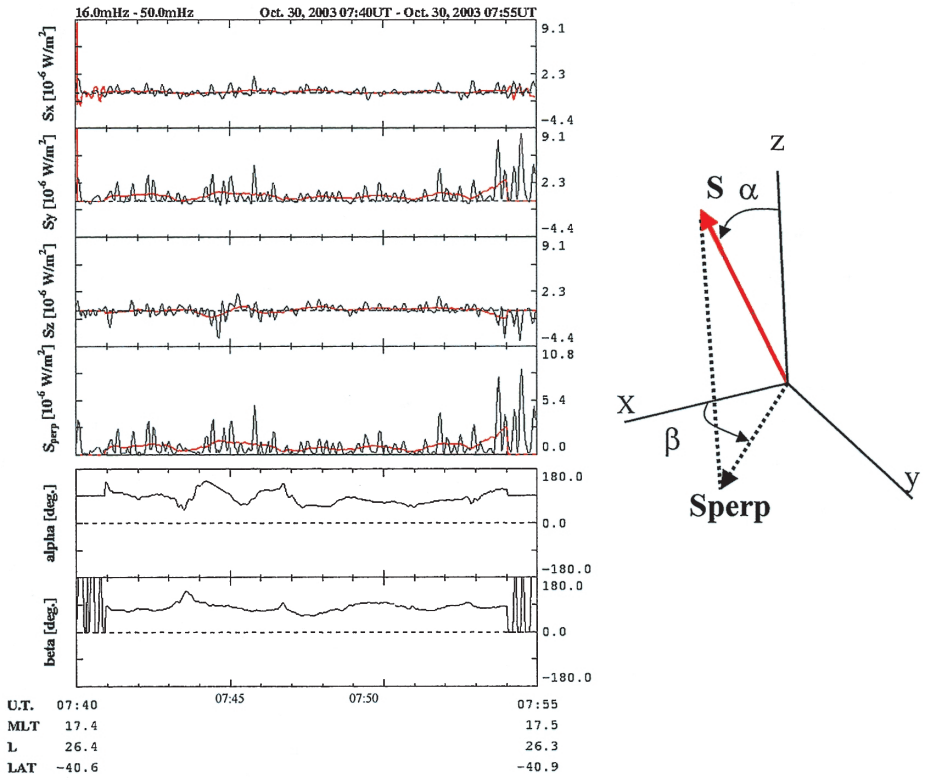

Fig. 15. Poynting flux of the Pc 3. From top to bottom the Poynting flux X, Y and Z-components, S_x, S_y and S_z, respectively, and the perpendicular component to the magnetic field, S_{perp}, and angles of Poynting flux respective to a direction of magnetic field, the polar angle, Alpha and the azimuth angle, Beta. The S_y component of the Poynting flux is superior to the others, and the Alpha = 90°, and the Beta = 90°, indicating that the Pc 3 wave energy propagates predominantly duskward perpendicular to the magnetic field-line.

Summarizing, on October 30, 2003 GEOTAIL traversed from the upstream region to the dusk-side outer magnetosphere through the magnetosheath. The amplitude of Pc 3 observed in these regions was very large, almost the same in the magnetosheath and in the outer magnetosphere, 6–8 nT, and amongst the largest ever observed in these regions. Usually the amplitude of Pc 3 is larger in the magnetosheath than in the outer magnetosphere, and the transmission rate is 10^{-2}–10^{-3}. However, in this case the amplitude of Pc 3 in the outer magnetosphere was almost the same to that observed in the magnetosheath. This might be due to the matching of several conditions of the solar wind in this storm period: the solar wind dynamic pressure was very large, the IMF B_z was very intense and northward throughout this interval.

The oscillation mode was different in the upstream, magnetosheath and outer magnetosphere regions. In the upstream region transverse oscillations were dominant and it may be generated by a cyclotron instability. On the other hand, in the

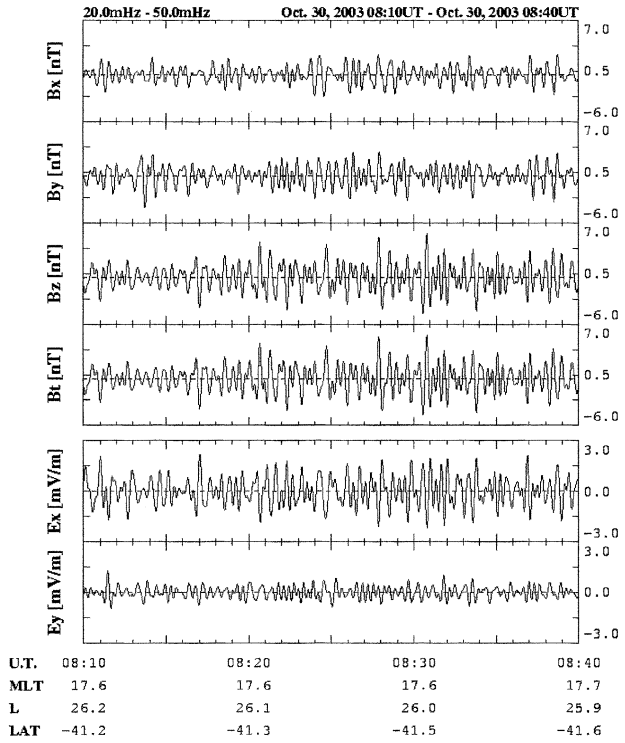

Fig. 16. A typical example of Pc 3 oscillations in the outer magnetosphere immediately after the magnetopause crossing. The compressional component of the magnetic field, B_z is superior to the other two transverse components, B_x and B_y. The amplitude of B_z is larger and extends to 6–7 nT on average.

magnetosheath near the magnetopause the oscillation changed to the compressional mode. The compressibility seemed to increase as the satellite approached the magnetopause. This might be due to the mixing of the conveyed cyclotron waves from the upstream region with the waves generated in the magnetosheath, where the mirror mode instability may be dominant as suggested by Anderson and Fuselier (1993), Anderson *et al.* (1994), Gray and Winske (1993), and Song *et al.* (1992, 1994). In the outer magnetosphere the compressional mode was dominant. This might be due to the transmission of the magnetosheath waves. The average direction of the Poynting flux was duskward, perpendicular to the average magnetic field, which indicates that Pc 3 wave energy in the dusk-side magnetosheath and the outer magnetoshere propagates duskward along with the draped duskward magnetic field and bulk flow in this region.

7. Summary and discussions

The primary importance in this study is that the causal relationship between the solar flares and their produced CMEs and the ICMEs, and their geo-effectiveness to the

terrestrial magnetosphere. The extremely large flares that occurred on October 28 and 29, 2003, produced extremely high-speed interplanetary coronal mass ejections and some of the largest magnetic field variations in the terrestrial magnetosphere ever recorded. A variety of enhanced activity was studied both in the space and on the ground. The observations by ACE and WIND revealed the peculiar magnetic and plasma structures in the interplanetary space in regions, upstream and downstream of the earth. The results from GEOTAIL clarified the properties of Pc 3 ULF waves from upstream and downstream of the bow shock, and in the dusk-side outer magnetosphere. The ground observations provide us a new insight into the dynamic response of the magnetosphere to these interplanetary disturbances. All of these contributed to establish a new perspective for the space weather prediction. The results from the examination of these satellite and ground observations during this super magnetic storm are summarized as follows:

1) Extremely high-speed solar wind hurled from the big flares was observed approximately as 2000 km/s.
2) The transit time of this high-speed solar wind from the sun to the earth was about 20 hrs.
3) This high-speed solar wind produced large amplitude magnetotail flapping motions.
4) A series of ICMEs yielded typical magnetic field rotations of the IMF, with the B_z component turnings of the north-south and south-north directions.
5) These IMF B_z polarization changes produced a typical response of the magnetic field activity of the terrestrial magnetosphere.
6) The southward orientation of the IMF, B_z produced substorm activities and large negative Dst variations extending to -350 nT and/or -400 nT, on the ground.
7) The northward orientation of the IMF, B_z enhanced magnetic pulsation activity in the magnetosphere.
8) During the northward IMF large amplitude Pc 5 oscillations were observed over the regions extending from the early morning to the pre-midnight, and from high to low latitude.
9) Enhanced Pc 3 wave activity was observed from the upstream region, through the magnetosheath, and to the dusk-side outer magnetosphere.
10) The amplitude of the Pc 3 was 4–5 nT in the upstream region, and 6–7 nT in the magnetosheath and the outer magnetosphere. These observed amplitudes are amongst the largest ever observed there.
11) Very high transmission efficiency of the Pc 3 waves from the magnetosheath to the outer magnetosphere was observed during this period.
12) The Poynting flux of the Pc 3 showed tailward propagation, dominantly perpendicular to the magnetic field-line.

A variety of magnetic field variations were examined in this study. First of all the transit time of the ICME was found to be surprisingly very short, about 20 hrs for both CMEs occurred on October 28, and 29, 2003. Gopalswamy *et al.* (2001) studied statistically the relationship between the transit time and the initial speed of the CME. However, they have no data for such a high solar wind speed in their study. The initial speeds of the CMEs occurred on October, 28 and 29, 2003 were approximately 2459 km/s, and 2029 km/s. Moreover, by comparing arrival times by ACE and WIND satellites

staying upstream of the bow shock and downstream in the distant tail, respectively, the speed for the first shock was estimated as 2189 km/s. The high speed of this shock suggests that the deceleration of the initial speed of CME is not effective to the distance of 1 AU. Therefore, the observed high initial speeds of CMEs for this October superstorm can not be directly compared with the result obtained by Gopalswamy *et al.* (2001). The relationship should be considered in more detail. This is our future work.

The relationship between transit times of super magnetic storms (Dst<-200 nT) and initial speeds of CMEs is shown in Fig. 1. This figure suggests that the observation of initial speed of CME is important for prediction of arrival time of super magnetic storms.

Tail flapping oscillations were observed in the very distant tail at $-160R_e$ in this study. Such a distant tail observation of flapping oscillations has never been reported. Much of the observation of the tail flapping motion reported so far were at most the distance to $-30\sim-60R_e$. The previous studies reported by Mihalov *et al.* (1970), Toichi and Miyazaki (1976), and Nishida and Lyon (1972) were based on satellite observations performed by Explorer 33, 34 and 35 within such distances. The typical characteristics of the flapping motion of the magnetotail reported by them were 3–8 min for the period and at most about 10 nT for the amplitude.

However, in this study the WIND satellite encountered the high-speed solar wind at the distant tail of about $-160R_e$ during this storm. The amplitude of the observed tail flapping motions was very large, about 30—40 nT. In general it is not considered that such large amplitude tail flapping motions might be due to the intrinsic geomagnetic field in such a distant tail. Therefore, the observed oscillations might be the magnetic field variations when they reconnected to the magnetic field of the ICMEs only in the X component.

The oscillations were observed only in the X component of the magnetic field. This means that the oscillation occurred alternately in the earthward and tailward oriented magnetic field in a X-Z plane. The amplitude of the alternate oscillations of the magnetic field was almost same. Therefore, the oscillation might be symmetric about the central line of the tail. Three decades ago Siscoe (1969) reported that there was a possibility of two types of the tail flapping oscillation in the magnetotail, *i.e.*, one is symmetric and the other is anti-symmetric. The observed characteristics in this study are in good agreement with the anti-symmetric oscillation mode since the magnetotail oscillated as a rigid oscillation of the outer boundaries about the center.

Large amplitude Pc 5 waves were observed during the recovery phase of the magnetic storm. This Pc 5 was characterized with a very coherent oscillation over widely spaced ground stations. The reason why such a coherent Pc 5 oscillation was observed might be due to the fact that it oscillated globally, like as a global mode, excited by a sudden compression of the magnetosphere due to the sudden enhancement of solar wind dynamic pressure, and the reason why the amplitude of the oscillation was very large might be due to the fact that it occurred during the intense northward IMF B_z, and also in the recovery phase of this super magnetic storm.

The condition of the magnetosphere during this period seemed to be very suitable for excitation of ULF waves. It has been well known that the Kelvin-Hermholtz

instability at the magnetospheric boundary is easily excited in such conditions (Miura, 1995). Moreover, the solar wind density was enhanced at that moment. This might be another important factor to trigger the Pc 5. This solar wind density enhancement was also observed by GEOTAIL. Large amplitude density oscillations were observed by GEOTAIL at the dawn side magnetopause. However, the period of the density oscillation observed by GEOTAIL was longer than that of the observed Pc 5 on the ground. At this moment the longitudinal location of GEOTAIL was almost similar to that of the IMAGE chain stations. Therefore, the oscillation observed on the ground might be of intrinsically magnetospheric origin and due to a global mode oscillation of the magnetosphere.

Another interesting observation during this storm period was Pc 3 oscillations observed in space by the GEOTAIL satellite, from upstream and downstream of the bow shock, and in the dusk-side outer magnetosphere. The observation was from 04 h UT to 09 h UT on October 30, when the north-south component of the IMF was completely northward with the intensity of 5–10 nT.

Surprisingly, the amplitude of the Pc 3 was almost the same in the magnetosheath and the outer magnetosphere. This was peculiar. Usually the amplitude of Pc 3 observed in the magnetosphere is much less than that observed in the magnetosheath. The transmission coefficient is known to be 1/100–1/1000. The reason for the present case might be due to the northward orientation of IMF, B_z.

Another important result concerns the oscillation characteristics of Pc 3. These varied from transverse oscillations observed in the upstream region to compressional oscillations near the magnetopause. The compressibility increased when the satellite approached the magnetopause. Anderson *et al.* (1994) reported the association of magnetic field fluctuations with the plasma depletion layer downstream of the quasi-perpendicular shock, mainly in the stagnation region, and found that there were two dominant spectral features. One was compressional fluctuations which related to the mirror mode instability, and the other was transverse fluctuations closely related to the cyclotron instability of H^+ and He^{2+}. They concluded that these magnetic field signatures and plasma properties were found to progress from mirror waves with high $\beta_{\|p}$ and low A_p in the magnetsheath proper to H^+ and He^{2+} cyclotron waves associated with the high A_p and low $\beta_{\|p}$ in the plasma depletion layer, where $\beta_{\|p}$ and A_p mean a beta ratio and an anisotropy factor, respectively. The above results in our study might be due to similar reasons discussed by Anderson *et al.* (1994).

In this study plasma data are not available to use due to the improper operation of low energy plasma instruments (LEP) onboard GEOTAIL during the storm period. Therefore, the plasma characteristics could not be identified in this study. However, both types of oscillations were observed in the magnetosheath. Therefore, they might correspond to the mirror waves and ion cyclotron waves, respectively.

Lee *et al.* (1988) studied a simulation of waves generated in the magnetosheath under the assumption of a high ion temperature anisotropy, from which they found that a large temperature anisotropy generates a mirror wave downstream of a quasi-perpendicular shock, and in the earth's bow shock large amplitude (perturbed B almost equal to B_0) mirror waves develop downstream of the shock ramp. The large amplitude Pc 3 waves observed in the magnetosheath might be supported by this simulation study.

Compressional mode oscillations dominated the transverse mode in the dusk side outer magnetosphere. This result is consistent with our previous study of Pc 3 oscillations using the GEOTAIL magnetic field observation for the satellite trajectory along with the dayside magnetopause, in which the compressional oscillation was dominant near the magnetopause boundary. When the satellite trajectory was separated from the magnetopause to the magnetosphere, the oscillation characteristics changed to the transverse oscillation and the signature of the field-line resonance was much clearly identified (Sakurai *et al.*, 1999).

8. Conclusion

The causal relationship between the solar flares and their produced magnetic field variations in the terrestrial magnetosphere can be studied on the basis of a variety of phenomenon observed in the interplanetary space, in the magnetosphere and on the ground during the period of the super magnetic storm occurred from October 29 to 31, 2003. The most important observation was the very high solar wind. The high stream solar winds successively produced big disturbances in the terrestrial magnetosphere. The period is the declining phase of the solar activity of the solar cycle 23. Why did such big flares occur during this phase? This question is most important to be resolved, but it remains still unresolved. However, we were able to obtain many valuable insights into the solar-terrestrial relationship throughout this study.

Acknowledgments

We have to acknowledge to use the SOHO LASCO CME CATALOG, which is generated and maintained by the Center for Solar Physics and Space Weather, The Catholic University of America in cooperation with the Naval Research Laboratory and NASA. SOHO is a project of international cooperation between ESA and NASA, and to use the magnetic field and plasma data measured by ACE, WIND, GOES 10 and GEOTAIL satellites through the Coordinated Data Analysis Web (CDAWeb). We also thank the institutes who maintain the IMAGE magnetometer array. The Dst index is due to the World Data Center C2 at the Kyoto University. We also thank the referees for their valuable comments on our original manuscript.

The editor thanks Drs. M. Nose and F.W. Menk for their help in evaluating this paper.

References

Anderson, B.J. and Fuselier, S.A. (1993): Magnetic pulsations from 0.1 to 4 Hz and associated plasma properties in the Earth's subsolar magnetosheath and plasma depletion layer. J. Geophys. Res., **98**, 1461–1479.

Anderson, B.J., Stephen, A., Fuselier, S.A., Gary, P. and Denton, R.E. (1994): Magnetic spectral signatures in the Earth's magnetosheath and plasma depletion layer. J. Geophys. Res., **99**, 5877–5891.

Gopalswamy, N., Lara, A., Yashiro, S., Kaiser, M.L. and Howard, R.A. (2001): Predicting the 1-AU arrival times of coronal mass ejections. J. Geophys. Res., **106**, 29207–29217.

Gray, S.P. and Winske, D. (1993): Simulations of ion cyclotron anisotropy instabilities in the terrestrial

magnetosheath. J. Geophys. Res., **98**, 9171–9179.
Lee, L.C., Price, P.P. and Wu, G.S. (1988): A study of mirror waves generated downstream of a quasi-perpendicular shock. J. Geophys. Res., **93**, 247–250.
Mihalov, J.D., Sonett, C.P. and Colburn, D.S. (1970): Reconnection and noise in the geomagnetic tail. Cosm. Electrodyn., **1**, 178–204.
Miura, A. (1995): Kelvin-Helmholtz instability at the magnetopause: Computer simulation. Physics of the Magnetopause, ed. by P. Song *et al.* Washington, D.C., Am. Geophys. Union, 285–291 (Geophysical Monograph 90).
Nishida, A. and Lyon, E.F. (1972): Plasma sheet at lunar distance structure and solar wind dependence. J. Geophys. Res., **77**, 4086–4099.
Sakurai, T., Tonegawa, Y., Kitagawa, T., Yumoto, K., Yamamoto, T., Kokubun, S., Mukai, T. and Tsuruda, K. (1999): Dayside magnetopause Pc 3 and Pc 5 ULF waves observed by the GEOTAIL satellite. Earth Planets Space, **51**, 965–978.
Siscoe, G.L. (1969): Resonant compressional waves in the geomagnetic tail. J. Geophys. Res., **74**, 6482–6486.
Song, P., Russell, C.T. and Thomsen, M.F. (1992): Waves in the inner magnetosheath: A case study. Geophys. Res. Lett., **19**, 2191–2194.
Song, P., Russell, C.T. and Gary, S.P. (1994): Identification of low-frequency fluctuations in the terrestrial magnetosheath. J. Geophys. Res., **99**, 6011–6025.
Toichi, T. and Miyazaki, T. (1976): Flapping motions of the tail plasma sheet induced by the interplanetary magnetic field variations. Planet. Space Sci., **24**, 147–159.